M. Howes and D. Morgan, Eds., *Charge-Coupled Devices and Systems*, John Wiley and Sons (1979).
S. Sze, *Physics of Semiconductor Devices*, John Wiley and Sons (1981).
J. Janesick, Ed., "Charge-coupled-device and charge-injection-device theory and application," *Optical Engineering* Vol. 26, No. 10, pp. 963–1067 (1987).
J. Janesick, Ed., "Charge-coupled-device manufacturer and application," *Optical Engineering* Vol. 26, No. 9, pp. 827–939 (1987).
J. Janesick, Ed., "Charge-coupled-device characterization, modeling, and application," *Optical Engineering* Vol. 26, No. 8, pp. 685–806 (1987).
C. Buil, *CCD Astronomy*, William-Bell, Inc. (1991).
L. Ristic, Ed., *Sensor Technology and Devices*, Artech House (1994).
A. Theuwissen, *Solid-State Imaging with Charge-Coupled Devices*, Kluwer Acad. Publishers, Dordrecht, Netherlands, ISBN 0-7923-3456-6 (4th print) (1995).
W. Leigh, *Devices for Optoelectronics*, Marcel Dekker, Inc. (1996).
J. Janesick and M. Blouke, "Sky on a chip: the fabulous CCD," *Sky and Telescope* Vol. 74, No. 3, pp. 238–242 (1987).
J. Kristian and M. Blouke, "Charge coupled devices in astronomy," *Scientific American* Vol. 247, No. 66 (1982).

CHAPTER 2

CCD TRANSFER CURVES AND OPTIMIZATION

2.1 CCD TRANSFER CURVES

Traditionally, CCD performance has been measured using commercial industry standards, which usually fall short of the requirements for many scientific digital applications. Also, scientific and commercial communities have been at odds with each other because each group uses different performance standards and units. This situation has created confusion as groups attempt to compare performance and data products. Commercial performance is often based on relative and photometric units (volts, lux, foot-candles, lumens, etc.), making it very difficult to know if absolute performance is being achieved. In contrast, scientific CCD camera systems are usually predicated on calibration standards that are based on absolute and physical radiometric units (photons, electrons, amps, watts, ergs, etc.). For example, it is physically meaningless to quote a noise or full well specification in relative units such as volts. However, these specifications become completely meaningful if specified in absolute units of electrons.

In characterizing the capabilities of the CCD for scientific work, numerous absolute test tools have been developed that allow performance to be expressed in absolute units. Test results from these techniques are often presented in the form of a transfer curve. For example, the spectral sensitivity for the CCD is graphed as absolute sensitivity as a function of wavelength, an important transfer curve called QE transfer. Different transfer curves describe different CCD and camera performance parameters measured under various test conditions. Transfer curves have been organized into three different working categories: (1) CCD performance, (2) CCD camera performance and (3) CCD camera calibration.

2.1.1 CCD PERFORMANCE

The first category of transfer curves, CCD performance, primarily serves the CCD manufacturer and customer. The curves form an important data baseline to aid in development of new CCD designs and fabrication processes. The curves are also used in the characterization and screening processes that grade sensors for quality and eventual component sale. The curves also form the basis of data sheets supplied to the customer.

Performance transfer curves are presented in two main groups, referred to as "mainstream" and "custom." Mainstream includes approximately a dozen curves that are universally applied by the manufacturer and custom designer. This chapter will review in considerable depth three very important mainstream performance transfer curves: photon transfer, x-ray transfer, and QE transfer. These three curves

Table 2.1 CCD performance parameters and transfer curves.

CCD Function	Performance Parameter	Transfer Curve or Image	Units
Charge Generation			
	Interacting QE	QE Transfer	interacting photons/incident photons
Charge Collection			
	Pixel nonuniformity	Photon Transfer	% nonuniformity
	Well capacity	Photon Transfer	e^-/pixel
	Charge collection efficiency	MTF	% modulation
Charge Transfer			
	Global CTE	X-ray Transfer	per pixel transfer
	Local CTE	Bar target image	
Charge Measurement			
	Sensitivity	Photon Transfer	Volts/e^-
	Linearity	Linearity Transfer	% nonlinearity
	Read noise	Photon Transfer	rms e^-
	Global dark current	Dark Current Transfer	e^-/sec/pixel
	Local dark current	Dark current image	

alone supply approximately 90% of the data required to make judgements about CCD performance. Table 2.1 tabulates these mainstream transfer curves into our four CCD operational categories: (1) charge generation, (2) charge collection, (3) charge transfer and (4) charge measurement.

There are literally hundreds of custom performance transfer curves to select from. Many of these curves will be presented in this book. Custom curves are generated under special testing conditions defined by the application at hand. For example, QE stability may be characterized in a form of a transfer curve under specific operating conditions. Such data was taken for the Hubble CCDs where 1% absolute photometric accuracy was required over a specified operating period.

2.1.2 CCD Camera Performance

The second group of transfer curves used to optimize CCD camera performance are listed in Table 2.2. For example, clock levels, dc bias voltages and clock wave shaping applied to the CCD are critical parameters characterized. The same curves define operating windows to maintain stable and reliable performance. Procedures presented at the end of this chapter will show how this optimization process is accomplished. Analog CCD signal processing circuits are also included in this group of transfer curves. For example, camera gain, offset, sample time, and bandwidth are critical parameters defined to achieve maximum signal-to-noise. These signal-processing parameters are discussed and specified in Chapter 6.

Table 2.2 CCD camera parameters and transfer curves.

Function	Performance Parameter	Transfer Curve	Units
CCD clock, bias and operating windows			
	Array threshold	OTG Transfer	
	Amplifier threshold	V_{DD} Transfer	Volts
	Inversion	OTG Transfer	Volts
	Well capacity	Photon Transfer	e^-/pixel
	Sensitivity	Photon Transfer	V/e^-
Clock wave-shaping			
	Well capacity	Photon Transfer	e^-/pixel
Signal processing			
	Offset	Photon Transfer	e^-
	Gain	Photon Transfer	e^-/DN
	Sample-to-sample time	Photon Transfer	sec
	CCD dominant time contant	Photon Transfer	sec

Table 2.3 CCD camera calibration parametrs and transfer curves.

Performance Parameters	Transfer Curve	Units
Signal-to-noise	Photon Transfer	Signal/Noise
Dynamic range	Photon Transfer	Full well/Noise
Linearity	Linearity Transfer	% nonlinearity
Quantum efficiency	QE Transfer	Interacting photons/incident photons
MTF	Modulation Transfer	% modulation
Bright cosmetics	Dark current image	
Dark cosmetics	Bar target image	
Camera Gain Constant	Photon Transfer	e^-/DN

2.1.3 CCD Camera Calibration

The third group of transfer curves used to calibrate a CCD camera system are tabulated in Table 2.3. Groups that procure off-the-shelf camera systems will find these curves essential. It is assumed that the two previous groups of transfer curves have been fully exercised before calibration takes place (i.e., Tables 2.1 and 2.2).

2.2 Photon Transfer

The photon transfer technique has proven to be one of the most valuable CCD transfer curves for calibrating, characterizing, and optimizing performance.[1,2] As described below, the photon transfer method is used to evaluate numerous CCD parameters in absolute terms. These parameters include read noise, dark current, quantum yield, full well, linearity, pixel nonuniformity, sensitivity, signal-to-noise, offset, and dynamic range. In addition, photon transfer is usually the first test per-

formed in determining the overall health of a new CCD camera system, because all camera hardware and software must be in perfect operating order. This includes the CCD, its clock and bias levels, signal processor, analog-to-digital converter (ADC), camera/computer interface circuits and the software behind data acquisition and image processing. Well-behaved photon transfer data imply that a camera system is capable of taking precise scientific measurements (e.g., absolute measurement errors typically less than 1% can be achieved). Also when camera problems do exist, photon transfer is usually the first diagnostic test tool called upon to identify subtle problems such as nonlinearity and noise issues. Photon transfer also gives—almost magically—the conversion constant used to convert relative digital numbers (DN) generated by the camera into absolute physical units of electrons. This very important conversion constant is referred to as the "camera gain constant," expressed in e^-/DN. The next section will show how photon transfer curves are generated and how this constant is found.

2.2.1 PHOTON TRANSFER DERIVATION

A schematic representation of a typical CCD camera is shown in Fig. 2.1. The camera can be described with five transfer functions, three that are related to the CCD (interacting QE, quantum yield and output amplifier sensitivity) and two associated with the off-chip signal processing circuitry (signal chain gain and ADC gain). The input to the camera is given in units of incident photons. The final output signal of the camera is achieved by encoding each pixel's signal into a digital number S(DN), typically using 8, 12 or 16 bits.

The output signal, S(DN), that results for a given exposure period is given by

$$S(\text{DN}) = P\,\text{QE}_I\,\eta_i\,S_V\,A_{CCD}\,A_1\,A_2, \tag{2.1}$$

where S(DN) represents the average signal for a group of pixels (DN), P is the average number of incident photons per pixel, QE_I is the interacting QE (interacting photons/incident photons), η_i is the quantum yield (the number of electrons generated, collected and transferred per interacting photon), S_V is the sensitivity of the sense node (V/e^-), A_{CCD} is the output amplifier gain (V/V), A_1 is the gain of the signal processor (V/V), and A_2 is the gain of the ADC (DN/V).

Example 2.1

Given Eq. (2.1), determine the average output signal S(DN) for a CCD camera with the following parameters.

$P = 1000$ photons/pixel
$\text{QE}_I = 0.5$
$\eta_i = 2\,e^-$/interacting photon

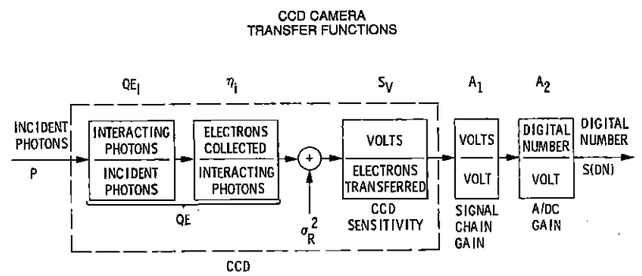

Figure 2.1 Block diagram of a typical CCD camera showing individual transfer functions.

$S_V = 10^{-6}$ V/e^-
$A_{CCD} = 0.8$ V/V
$A_1 = 100$ V/V
$A_2 = 2^{16}$ DN/V.

Solution:
From Eq. (2.1),

$$S(\text{DN}) = 1000 \times 0.5 \times \left(2 \times 10^{-6}\right) \times 0.8 \times 100 \times 2^{16},$$

$$S(\text{DN}) = 5240\,\text{DN}.$$

As mentioned above, to convert the output signal DN into fundamental physical units, it is necessary to find the appropriate factors in converting DN units to either interacting photons or signal electrons generated. The constants which accomplish this conversion are defined by

$$K = \frac{1}{S_V\,A_{CCD}\,A_1\,A_2} \tag{2.2}$$

and

$$J = \frac{1}{\eta_i\,S_V\,A_{CCD}\,A_1\,A_2}, \tag{2.3}$$

where K and J are camera gain constants given in units of e^-/DN and interacting photons/DN respectively. Note that these equations are related through the quantum yield, η_i, by

$$\eta_i = \frac{K}{J}. \tag{2.4}$$

It is possible to determine the constants J and K by measuring each transfer function indicated in Fig. 2.1 separately and then combining these results as in Eqs. (2.2) and (2.3). However, it is difficult to measure each CCD parameter precisely (QE_I, η_i, and S_V). Instead, the photon transfer technique will determine J and K to any desired precision without knowledge of the individual transfer functions.

To evaluate the constant K, the CCD is stimulated with photons that generate single e-h pairs. Recall from Chapter 1 that wavelengths > 4000 Å generate single e-h pairs (i.e., $\eta_i = 1$). Wavelengths < 4000 Å are more energetic and generate multiple e-h pairs. Assuming a unity quantum yield, Eq. (2.1) can be rewritten as

$$S(\text{DN}) = \frac{P_I}{K}, \tag{2.5}$$

where P_I is the number of interacting photons per pixel [i.e., $P_I = (QE_I)(P)$].

The constant K can now be determined by relating the output signal to its variance, $\sigma_S^2(\text{DN})$. The variance of Eq. (2.5) is found using the propagation of errors formula,

$$\sigma_S^2(\text{DN}) = \left[\frac{\partial S(\text{DN})}{\partial P_I}\right]^2 (\sigma_{P_I}^2) + \left[\frac{\partial S(\text{DN})}{\partial K}\right]^2 (\sigma_K^2) + \sigma_R^2(\text{DN}), \tag{2.6}$$

where we have added in quadrature the output amplifier read noise floor variance $\sigma_R^2(\text{DN})$, as indicated in Fig. 2.1.

Performing the required differentiation on Eq. (2.5) and assuming that the constant K has a negligible variance (i.e., $\sigma_K^2 = 0$), the variance in $S(\text{DN})$ is found:

$$\sigma_S^2(\text{DN}) = \left(\frac{\sigma_{P_I}}{K}\right)^2 + \sigma_R^2(\text{DN}). \tag{2.7}$$

Using $\sigma_{P_I}^2 = P_I$ (photon statistics) and Eq. (2.5),

$$K = \frac{S(\text{DN})}{\sigma_S^2(\text{DN}) - \sigma_R^2(\text{DN})}. \tag{2.8}$$

Equation (2.8) is a very important expression and can be used, without any further calibration, to convert output noise and signal measurements in DN directly into units of electrons. We will demonstrate below how useful this result is.

For wavelengths longer than 4000 Å, the constants K and J are equal since the quantum yield is unity. The constant J is also found by relating the output signal given by Eq. (2.3) to its variance. Using the propagation of errors formula and assuming that the quantum yield has no variance, we find

$$J = \frac{S(\text{DN})}{\sigma_S^2(\text{DN}) - \sigma_R^2(\text{DN})}, \tag{2.9}$$

where J gives the number of interacting photons/DN.

Equations (2.8) and (2.9) form the basis for the photon transfer technique. By simply measuring the mean signal and its variance both for visible photons and for photons at any other specific wavelength of illumination (i.e., $\lambda < 4000$ Å), the values K and J can be determined. Once the constants K and J are known, the quantum yield for photons at the wavelength under consideration can be determined through Eq. (2.4).

Example 2.2

Find the constant K when a CCD is stimulated with visible light. Assume the following measurement parameters: $S(\text{DN}) = 4000$ DN, $\sigma_S^2(\text{DN}) = 300$ DN rms, and $\sigma_R^2(\text{DN}) = 10$ DN.

Solution:

From Eq. (2.8),

$$K = 4000/(300 - 10),$$

$$K = 13.79\,\text{e}^-/\text{DN}.$$

2.2.2 PHOTON TRANSFER CURVE

The photon transfer curve illustrated in Fig. 2.2 is a response from a CCD that is uniformly illuminated at different levels of light. We plot noise or the standard deviation, $\sigma_S(\text{DN})$, as a function of average signal, $S(\text{DN})$, for a group of pixels contained on the CCD array. Data is plotted on a log–log scale in order to cover the large dynamic range of the CCD. Three distinct noise regimes are identified in the plot. The first regime, the read noise floor $\sigma_R(\text{DN})$, represents the random noise measured under totally dark conditions. This noise is ultimately limited by on-chip amplifier noise, but can represent any other noise sources that are independent of the signal level (e.g., shot noise generated by dark current).

As the illumination to the CCD is increased, the noise becomes dominated by the shot noise of the signal, shown in the middle region of the curve. Shot noise is the noise associated with the random arrival of photons on the CCD. Some pixels intercept more photons than others, which accounts for the variance seen in pixel values. Since the plot shown is on log coordinates, the shot noise is characterized by a line of slope 1/2. This specific slope arises because the uncertainty in the

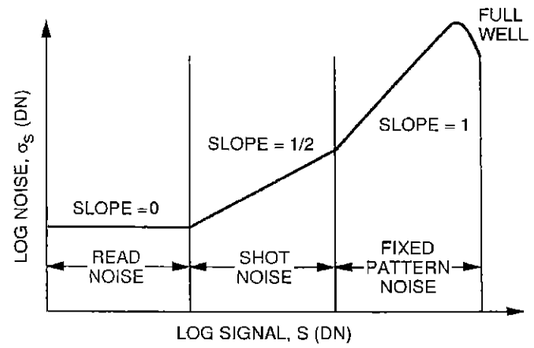

Figure 2.2 Total noise photon transfer curve illustrating three noise regimes over the dynamic range of the CCD.

quantity of charge collected in any given pixel is proportional to the square root of the number of incident photons (as governed by Poisson's statistics).

The third regime is associated with fixed-pattern or pixel nonuniformity noise that results from sensitivity differences among pixels. Pixel nonuniformity is a manifestation of processing variations and photomask alignment errors when the CCD is fabricated. This problem generates pixels with different responsivities. Pixel nonuniformity noise is proportional to signal and consequently produces a characteristic slope of unity on our plot.

The onset of full well is observed at some illumination level within the fixed-pattern noise regime and is seen as a break in the slope of one. At this point the charge spreads between pixels (i.e., blooming), smoothing and lowering the noise component as seen in the plot. This action causes the noise value to suddenly decrease, making full well obvious (the signal component remains high).

Figure 2.3(a) shows a photon transfer curve generated by a backside-illuminated $800 \times 800 \times 15$-μm CCD using a 20×20 subarray of pixels that are uniformly illuminated with visible light (7000 Å). We refer to the curve as "classical" because pixel nonuniformity has been removed, a simple computer process step that will be described in this section. The curve is generated by varying the exposure sequence beginning with a dark frame (i.e., CCD not exposed to light). Then the exposure time is increased and signal level is measured in DN units until saturation is reached. Exposure periods are typically increased logarithmically to cover the entire dynamic range of the CCD. The exposure period is the time period when a shutter is open or how long the CCD is exposed to the light source. Usually the integration period is fixed during a photon transfer sequence. In this manner, only the exposure time is varied, allowing the total frame time period (integration + read out) to be fixed. Figure 2.3(b) shows another photon transfer curve which exhibits a much greater dynamic range.

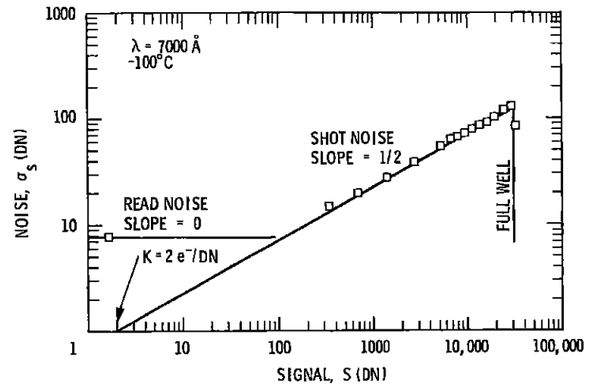

Figure 2.3(a) Photon transfer curve generated by a WF/PC I 800 × 800 CCD with pixel nonuniformity removed.

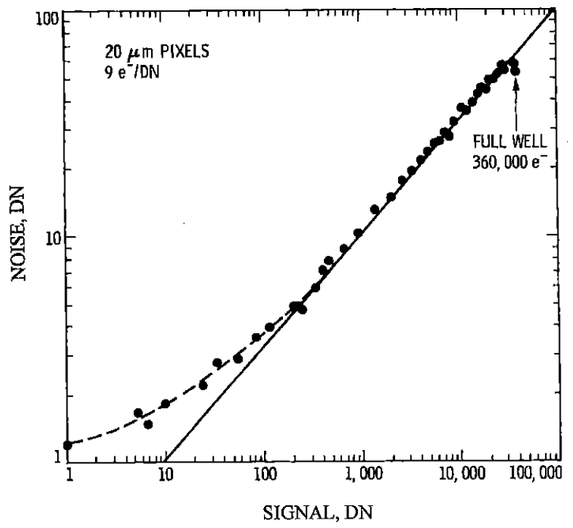

Figure 2.3(b) Photon transfer for a CCD that exhibits a wide dynamic range.

It should be mentioned that a simple LED placed in front of the CCD can be pulsed to expose the sensor, again leaving the integration period fixed. The signal charge generated will be proportional to the time the LED is "on." Also, an

LED can be turned "on" and "off" very quickly, allowing for very short exposure times (on the order of a microsecond). In contrast, mechanical shutters are limited to exposure times no shorter than 1 msec. For these shuttered systems, a 10-sec integration period may be required to cover a signal dynamic range of 10^4, which is often encountered in CCD work. On the other hand, the LED stimulus would only require a maximum of 10 msec, thus shortening the time to take data.

The abscissa $S(\text{DN})$ is proportional to the exposure period or the average number of incident photons and photo-generated charge per pixel element. The 400 pixel values are averaged, yielding $S(\text{DN})$, after a fixed average electrical offset is subtracted from each pixel. That is,

$$S(\text{DN}) = \frac{\sum_{i=1}^{N_{pix}} [S_i(\text{DN})]}{N_{pix}} - S_{OFF}(\text{DN}), \tag{2.10}$$

where $S_i(\text{DN})$ is the signal value of the ith pixel (DN), N_{pix} is the number of pixels contained in the subarray, and $S_{OFF}(\text{DN})$ is the average offset level (DN).

The offset, $S_{OFF}(\text{DN})$, represents the camera's output DN level in total absence of signal electrons. Subtracting a precise offset is an important requirement in measuring signal levels. Offset can sometimes be determined from a dark exposure using pixels from the same pixel region where signal is measured. However, the offset information on the array may be corrupted with dark current or other sources of charge (e.g., light leak, spurious charge, etc.). The best location on the CCD for a zero signal level is in the "extended pixel region" of the horizontal register (see Fig. 1.12). Extended pixels are found at the beginning of a line or are purposely created by overclocking the horizontal register. In the latter case, those pixels following the last video pixel represent a good measurement of zero charge. Extended pixels should therefore always accompany video pixels as they are stored in a computer. In the case of the Wide Field/Planetary Camera, one extended pixel for every video line of data is sent back to Earth for offset information. It is very important to track the offset level because it can change from frame to frame. Sensitive image-processing programs (e.g., flat fielding and nonlinearity measurements) require an offset accuracy of better than 1 DN. Note from Eq. (2.10) that the offset level does not need to be subtracted pixel by pixel. Only a single difference from the average signal level is required, thus saving computing time.

Noise data for the ordinate are found by calculating the standard deviation of the 400 pixels after pixel-to-pixel nonuniformity is removed. Pixel nonuniformity is eliminated by simply differencing, pixel by pixel, two identical images taken back to back at the same exposure level. The variance, $\sigma_S^2(\text{DN})$, of this differenced frame is given by

$$\sigma_S^2(\text{DN}) = \frac{\sum_{i=1}^{N_{pix}} [S_i(\text{DN}) - S(\text{DN})]^2}{2N_{pix}}. \tag{2.11}$$

Note that a factor of two must be included in the denominator of Eq. (2.11) because the noise power increases by two within the differenced frame. In other words, when two identical frames are either subtracted (as in this case) or added, the random noise component (rms or standard deviation) of the resultant frame increases by the square root of two.

To improve statistics for photon transfer data, three or more exposures at the same signal level can be taken. $S(\text{DN})$ is then found by taking the average of the three mean levels measured. The noise, $\sigma_S(\text{DN})$, is determined by first differencing frames 1 & 2, then frames 2 & 3, and lastly frames 1 & 3, and generating three standard deviations. These values are then averaged together, yielding $\sigma_S(\text{DN})$. This is the method used in generating the photon transfer curves in Fig. 2.3. One can also take a larger region of interest from the CCD (that is, greater than 20×20 pixels) to improve statistics, as long as the region selected does not contain blemish artifacts (multiple frames were required when early CCDs exhibited cosmetic problems).

It should also be mentioned that dark current, if it exists, does not need to be subtracted from the signal level. This is because dark charge only adds to the signal charge measured. It is not important in the photon transfer technique how charge is generated, as long as the source exhibits shot noise characteristics, which is the case for dark current (refer to Chapter 7). In fact, a photon transfer curve can be generated using only thermally generated dark current; i.e., no light source is required. However, if total noise is plotted as in Fig. 2.2 without frame differencing, dark nonuniformity will dominate the noise term with very little shot noise seen. Pixel-to-pixel dark current nonuniformity for CCDs is typically 10% rms of the average signal level, compared to pixel-to-pixel sensitivity nonuniformity, which is approximately 1%.

2.2.3 CAMERA GAIN CONSTANTS

The conversion factors K and J can be found graphically or precisely through Eqs. (2.8) and (2.9) by measuring $S(\text{DN})$ and $\sigma_S^2(\text{DN})$ at a signal level where $\sigma_S^2(\text{DN}) \gg \sigma_R^2(\text{DN})$. The graphical approach will be examined in this section to obtain approximate values. For example, the constant K for the photon transfer curve shown in Fig. 2.3(a) is found by extending the slope 1/2 line back to the x axis intercept corresponding to $\sigma_S(\text{DN}) = 1$ DN. The intercept on the signal axis represents the value K [i.e., $K = S(\text{DN})$]. This remarkable result can be proven by taking the logarithm of Eq. (2.8), yielding

$$\log[K] = \log[S(\text{DN})] - \log\left[\sigma_S^2(\text{DN}) - \sigma_R^2(\text{DN})\right]. \tag{2.12}$$

We next assume $\sigma_R(\text{DN}) = 0$ since the slope 1/2 curve is shot noise limited. Then we let $\log[\sigma_S(\text{DN})] = 0$ since $\sigma_S(\text{DN}) = 1$. Substituting these values reduces the above equation to $K = S(\text{DN})$, the desired result.

Example 2.3

Determine graphically the camera gain constant K for the photon transfer curve shown in Fig. 2.3(a). Then determine the read noise and full well for the sensor in units of electrons. Also find the read noise and full well for the photon transfer curve shown in Fig. 2.3(b).

Solution:

Figure 2.3(a):

The signal intercept for the shot noise curve is approximately $K = 2.0\,e^-/DN$ as shown. Therefore, the 8 DN rms of noise corresponds to a read noise of $16\,e^-$ rms. Saturation occurs at 30,000 DN, which corresponds to a charge capacity of $60{,}000\,e^-$.

Figure 2.3(b):

The camera gain constant in Fig. 2.3(b) is $9\,e^-/DN$. The 40,000 DN saturation level corresponds to a full well of $360{,}000\,e^-$. The read noise of 1 DN is $9\,e^-$ rms.

The same approach can be used in determining the constant J when the quantum yield is greater than 1. Since S_v, A_1, and A_2 are constant for a given CCD camera system, a decrease in K can be directly attributed to an increase in the quantum yield (i.e., multiple electron/hole pairs per interacting photon). For example, Fig. 2.4 shows three photon transfer curves that are generated by a backside-illuminated 800 × 800 CCD. The curves show the response of the CCD when exposed to light of the following wavelengths: (1) red light (7000 Å), (2) UV light (1216 Å) and (3) soft x rays (2.1 Å). The corresponding intersections on the signal axis using the graphical approach for these wavelengths are, respectively, $K = 2.3\,e^-/DN$, $J = 0.77$ and $J = 1.62 \times 10^{-3}$ interacting photons/DN.

Example 2.4

Determine the quantum yield for the three photon transfer curves presented in Fig. 2.4.

Solution:

7000 Å (1.77 eV):

Stimulating the CCD with 7000-Å light generates single electron-hole pairs yielding a signal intercept value of $K = 2.3\,e^-/DN$.

1216 Å (10.2 eV):

At this wavelength, multiple electron-hole pairs are generated, causing the photon transfer curve to shift to a smaller signal intercept value (i.e., from 2.3 to 0.77). The quantum yield is found from Eq. (2.4).

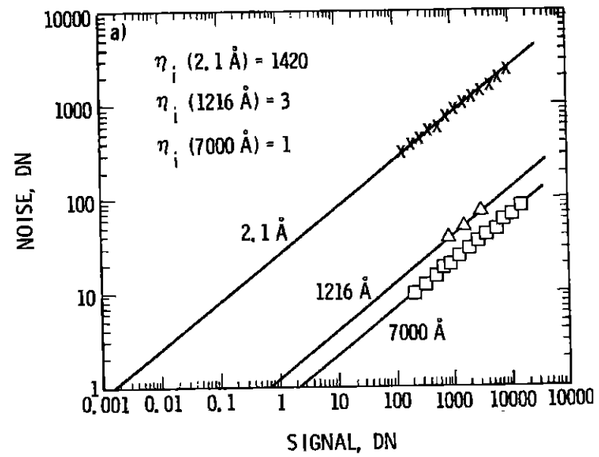

Figure 2.4 Three photon transfer curves taken at 7000 Å, 1216 Å and 2.1 Å.

$$\eta_i = 2.3/0.77,$$

$$\eta_i = 2.99\,e^-/\text{interacting photon}.$$

2.1 Å (5.9 keV):

The intercept shifts to 1.6×10^{-3} when the CCD is stimulated with soft x rays. The quantum yield is

$$\eta_i = 2.3/(1.62 \times 10^{-3}),$$

$$\eta_i = 1420\,e^-/\text{interacting photon}.$$

The quantum yield for x-ray interaction always falls short of the ideal quantum yield, η_i (i.e., $5900/3.65 = 1620\,e^-$). This result is because photogenerated charge generated by the x-ray photon is collected in more than one pixel, thus reducing the measured quantum yield (referred to as split x-ray events). This effect is associated with charge collection efficiency, discussed in Chapter 4.

2.2.4 CAMERA GAIN HISTOGRAM

The graphical method of determining K and J above is accurate to within 10–20%, depending upon how well the data points on the "slope 1/2 line" are fitted to a straight edge. The constant K can be determined precisely by repeatedly measuring S(DN) and σ_S^2(DN) and inserting these values into Eq. (2.8). If many different 20×20 subarrays over the CCD are interrogated, a "camera gain histogram" for K, as shown in Fig. 2.5, can be generated. This is accomplished by storing two flat-field frames taken near full well to assure that read noise is negligible. The two frames are then subtracted pixel by pixel to remove pixel nonuniformity, to obtain σ_S^2(DN). Then, a 20×20 subarray is randomly selected from the stored data and Eq. (2.8) is applied, yielding a value for K. A different 20×20 region is then randomly selected and the process repeated for another K value. As values of K are generated in this fashion, they are plotted in histogram form. The distribution is normal and weighted about the mean value of K. The histogram technique allows one to measure the camera gain constant to any desired level of precision.

By incorporating many 20×20 pixel subarrays into the histogram, those regions on the device that contain blemish artifacts (e.g., column blemishes, blocked channels, etc.), which would give an erroneous value of K, can be eliminated. Areas on the CCD that are not well behaved are usually recognized as data points outside the main histogram peak (three of these points are seen in Fig. 2.5).

A similar histogram can be generated to measure the quantum yield, η_i (i.e., K/J). In this case, four frames of data are required: two visible frames to determine K and two frames at a specific wavelength of interest (< 4000 Å). For example, Fig. 2.6 presents two photon transfer histograms for a frontside-illuminated

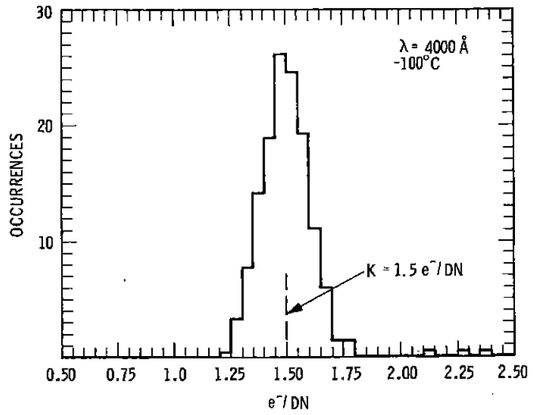

Figure 2.5 Camera gain histogram derived from photon transfer data.

CCD stimulated with 7000 Å light and 2.1 Å soft x rays. The histograms are generated by employing Eqs. (2.8) and (2.9) as before. The quantum yield for soft x rays is $790\,e^-$ (K/J), less than the ideal response ($1620\,e^-$) for reasons explained above.

Figure 2.7(a) shows quantum yield measurements taken in the UV with a backside-illuminated CCD. These data were produced by generating histograms for selected wavelengths as in Fig. 2.6. For example, Fig. 2.7(b) shows two histograms taken at 6400 Å and 2400 Å and the shift in e^-/DN that occurs between these two wavelengths.

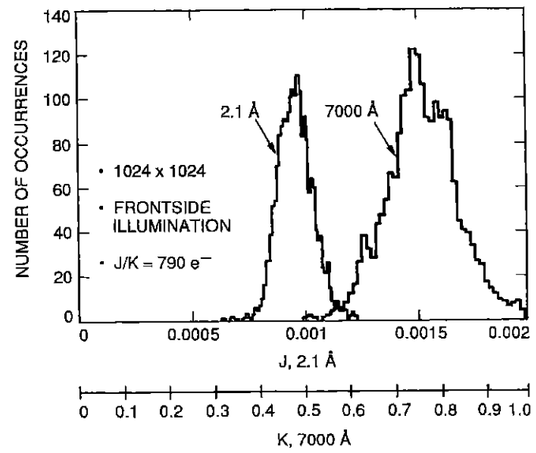

Figure 2.6 Two camera gain histograms generated at 7000 Å and 2.1 Å.

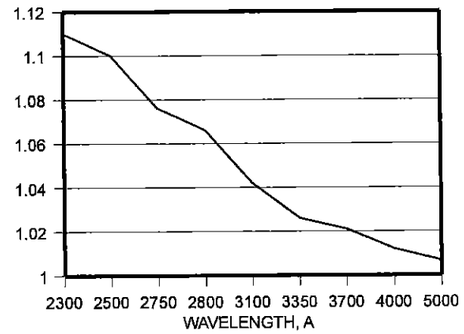

Figure 2.7(a) Quantum yield as a function of wavelength.

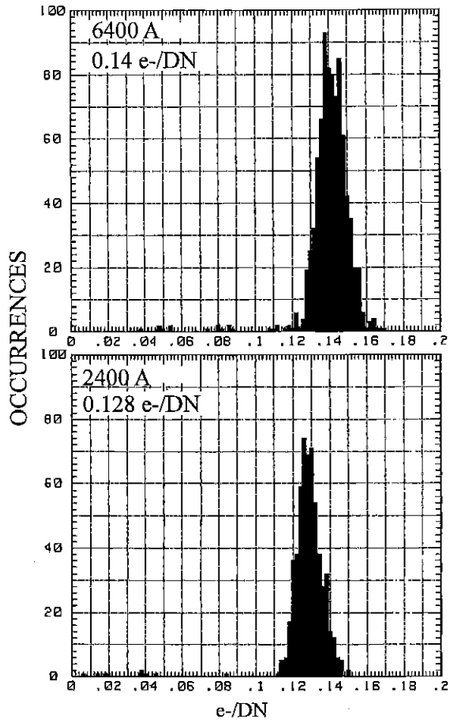

Figure 2.7(b) Quantum yield histograms used in Fig. 2.7(a).

2.2.5 Camera Gain Uncertainty

The variance of K is found by applying the propagation of errors formula to Eq. (2.8) rewritten in the form

$$K = \frac{S(\text{DN})}{N(\text{DN})^2}, \tag{2.13}$$

where $N(\text{DN}) = \sigma_S(\text{DN})$. Note that we have assumed that read noise, σ_R, is negligible.

Applying the propagation of errors formula to this equation yields

$$\sigma_K^2 = \left[\frac{\partial K}{\partial S(\text{DN})}\right]^2 (\sigma_S^2) + \left[\frac{\partial K}{\partial N(\text{DN})}\right]^2 (\sigma_N^2). \tag{2.14}$$

Assuming photon statistics (i.e., $K\sigma_S(\text{DN}) = [K\,S(\text{DN})]^{1/2}$), the uncertainty in the signal measured is

$$\sigma_S^2 = \frac{S(\text{DN})}{K N_{pix}}. \tag{2.15}$$

The uncertainty in noise measured is

$$\sigma_N^2 = \frac{N(\text{DN})^2}{2N_{pix}}. \tag{2.16}$$

Performing the differentiation required to evaluate Eq. (2.14) and substituting these two equations yields

$$\sigma_K^2 = \frac{1}{N(\text{DN})^4}\frac{S(\text{DN})}{K N_{pix}} + \frac{4S(\text{DN})^2}{N(\text{DN})^6}\frac{N(\text{DN})^2}{2N_{pix}}. \tag{2.17}$$

Applying Eq. (2.13) simplifies this equation into

$$\sigma_K^2 = \frac{1}{N_{pix}}\left[K\left(\frac{1}{S(\text{DN})} + 2K\right)\right]. \tag{2.18}$$

As long as $\sigma_S(\text{DN}) \ll S(\text{DN})$, which will be true for reasonable signal levels, we can use the approximation $1/S(\text{DN}) \ll 2K$, reducing Eq. (2.18) to the final result,

$$\sigma_K = \left[\frac{2}{N_{pix}}\right]^{1/2} K. \tag{2.19}$$

It is interesting to note that the uncertainty of K is independent of signal level as long as the read noise is negligible and the signal level is large compared to the shot noise. Equation (2.19) has been experimentally confirmed with good precision.

Example 2.5

Determine the uncertainty (rms) of the camera gain constant when sampling a 20×20 pixel region, when $K = 5\,\text{e}^-/\text{DN}$.

Solution:

$$\sigma_K = 5 \times (2/400)^{1/2},$$

$$\sigma_K = 0.35\,\text{e}^-/\text{DN rms}.$$

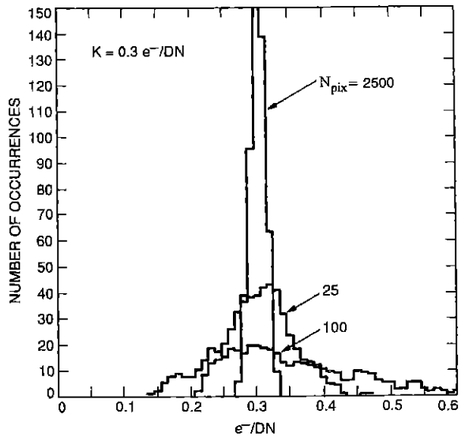

Figure 2.8(a) Camera gain variance as a function of pixels sampled.

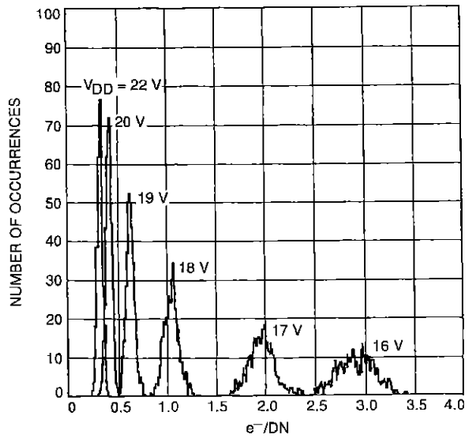

Figure 2.8(b) Camera gain histograms taken at different V_{DD} potentials.

Figure 2.8(a) presents three camera gain histograms showing that the variance of K decreases with increasing N_{pix}. Figure 2.8(b) plots camera gain histograms for different drain voltages (V_{DD}) to the on-chip amplifier. As V_{DD} is lowered, the CCD gain, A_{CCD}, decreases, causing K to increase and the histogram width to broaden.

2.2.6 DYNAMIC RANGE

Well capacity and read noise specify the dynamic range of the CCD using

$$\mathrm{DR} = \frac{S_{FW}(\mathrm{e}^-)}{\sigma_R(\mathrm{e}^-)}, \tag{2.20a}$$

where $S_{FW}(\mathrm{e}^-)$ is full well.

Dynamic range can also be expressed in decibels (dB) as

$$\mathrm{DR} = 20\log\left(\frac{S_{FW}(\mathrm{e}^-)}{\sigma_R(\mathrm{e}^-)}\right). \tag{2.20b}$$

Example 2.6

Apply Eq. (2.20) to Example 2.3 and find the dynamic range for the CCD characterized in Fig. 2.3(a). Also, express dynamic range in decibels.

Solution:

From Eq. (2.20a),

$$\mathrm{DR} = 60{,}000/16,$$

$$\mathrm{DR} = 3{,}750.$$

From Eq. (2.20b),

$$\mathrm{DR} = 20 \times \log(60{,}000/16),$$

$$\mathrm{DR} = 71.48\,\mathrm{dB}.$$

The enormous dynamic range that the CCD exhibits cannot usually be represented properly when images are printed and displayed. For example, photographic film at its "spatial resolution limit" (approximately 5 μm) can only resolve 10 to 20 shades of gray. In comparison, a 5-μm pixel CCD can differentiate hundreds of levels at its spatial limit (i.e., Nyquist). The dynamic range for film and the CCD are compared in Fig. 2.9(a) using several images of a globular star cluster field. Each 8-bit image shown is derived from a single 16-bit CCD exposure. For example, the image shown in the upper right-hand corner uses the most significant 8 bits, with the least significant 8 bits dropped. Note that only the brightest stars that are near full well are seen. The picture presented in the lower left-hand corner uses the least significant 8 bits. The central region of the cluster is saturated because of

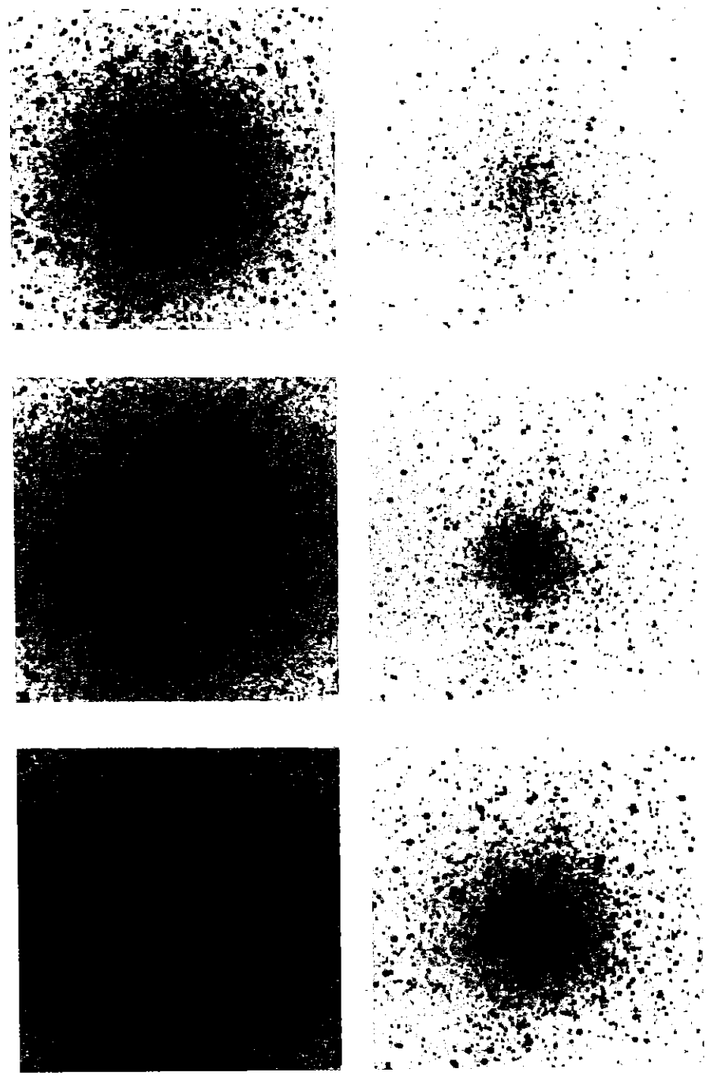

Figure 2.9(a) A globular star cluster image demonstrating the wide dynamic range of a CCD.

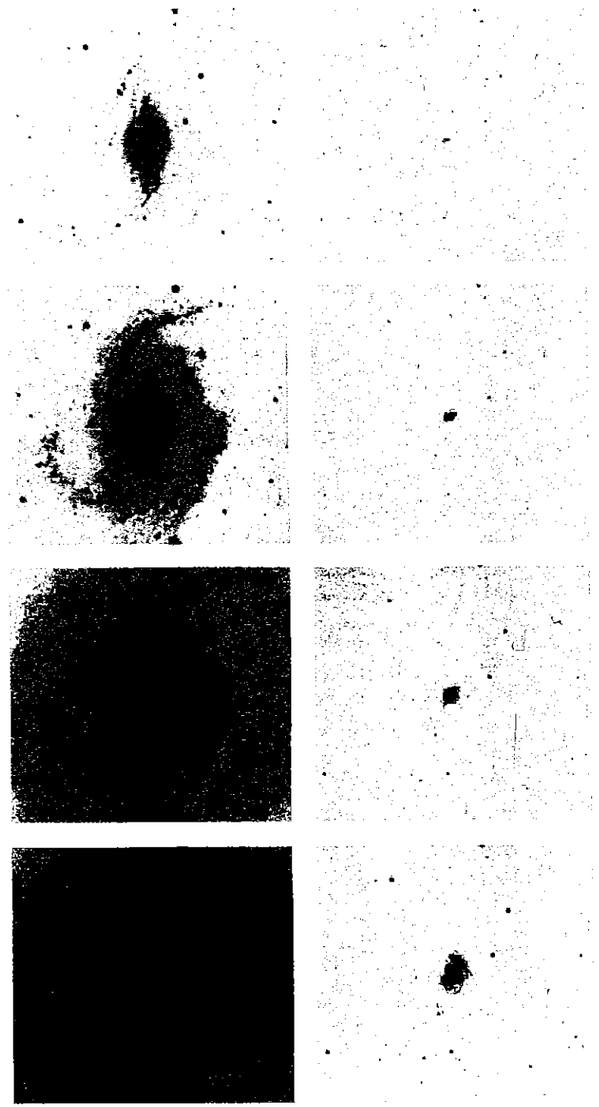

Figure 2.9(b) Galaxy image processed as Fig. 2.9(a).

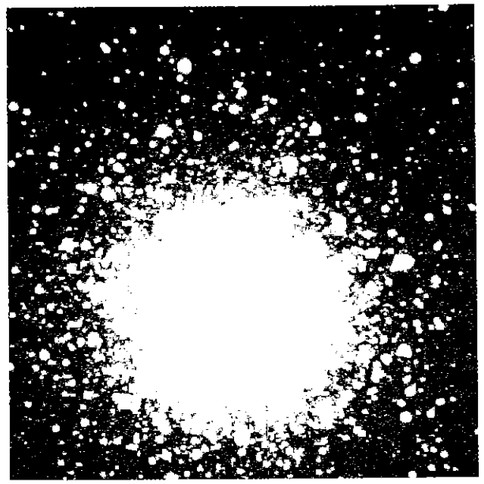

Figure 2.10(a) Gobular star cluster showing saturation within center region.

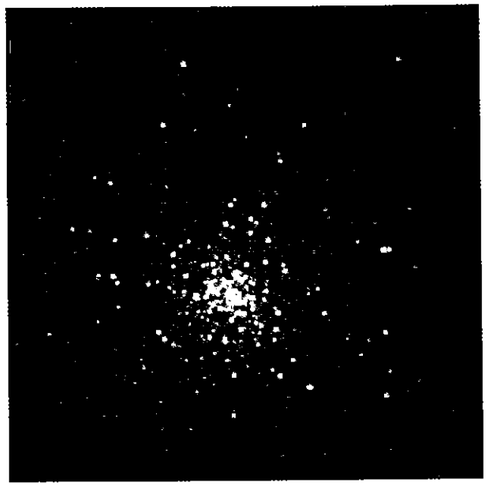

Figure 2.10(b) Same gobular star cluster printed logarithmically.

the limited dynamic range of the film. Figure 2.9(b) shows a picture of a galaxy, again demonstrating the dynamic range of the CCD.

Figure 2.10 demonstrates a compression technique that allows the CCD's full dynamic range to be better presented on film. Figure 2.10(a) shows a globular cluster star field, showing the least significant 8 bits. Figure 2.10(b) was produced by using a logarithmic gain adjustment on each pixel value, compressing information to match the dynamic range of the film. Now stars can be seen without saturating the central region of the cluster.

2.2.7 LINEARITY

Nonlinearity is a measurement of the camera gain constant as a function of signal. Ideally there should be no dependence. Any gain change with signal is important to scientific applications where absolute measurements are taken. For example, in astronomy, a star's brightness is usually determined by comparing its brightness to a "standard star" whose brightness is already known. The error (or nonlinearity) for this measurement is equal to the gain (i.e., e^-/DN) ratio of the stars signal levels. The nonlinearity specification for WF/PC is $< 1\%$ over the dynamic range of the camera system. This means that the absolute brightness for an unknown star will be accurate to within 1%.

The same nonlinearity error is measured using photon transfer data by plotting signal as a function of exposure time. In general, the output signal, S(DN), as a function of exposure time can be expressed in a power series as

$$S(\text{DN}) = C(t_E)^{\gamma}, \tag{2.21}$$

where C is a proportionality constant, t_E is the exposure time (sec), and γ is a measure of the linearity of the device. A gamma of unity signifies that the CCD output signal is proportional to exposure time.

Figure 2.11(a) presents a linearity transfer curve of S(DN) as a function of exposure time on log-log coordinates. The straight line of a unity slope indicates good linearity (i.e., $\gamma = 1$). As can be seen, linearity is exceptional for the CCD as compared to other types of imaging sensors (e.g., film, vidicon tubes). To measure nonlinearity at the 1% level, a different transfer curve is used. Figure 2.11(b) presents the "linearity residuals" which expand the results of Fig. 2.11(a) using the equation

$$LR = 100\left(1 - \frac{S_M(\text{DN})/t_{EM}}{S(\text{DN})/t_E}\right), \tag{2.22}$$

where LR is the linearity residual at a specific signal level (%). The variables S(DN) and t_E are the signal (DN) and exposure time (sec) measured in the photon transfer process, and t_{EM} is the exposure time required to produce a signal (sec), S_M, at mid-scale in the plot (DN).

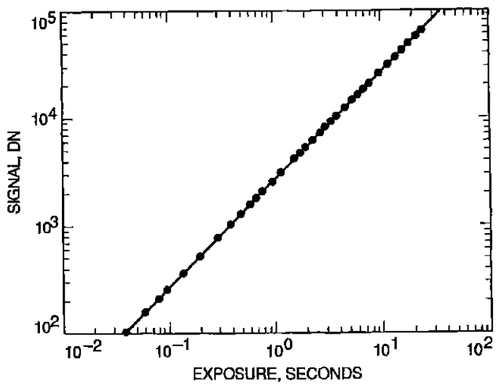

Figure 2.11(a) Linearity transfer curve.

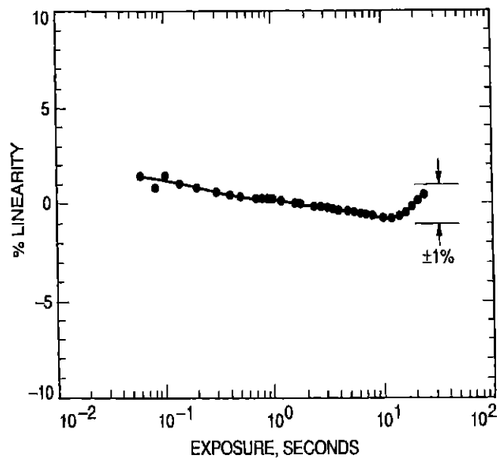

Figure 2.11(b) Linearity residual transfer curve that exhibits nonlinearity $< 1\%$ over the sensor's dynamic range.

Example 2.7

Find the linearity residual at an output signal of 4900 DN for an exposure period of 0.5 sec. Assume a mid-scale level of 10^4 DN at 1-sec exposure time.

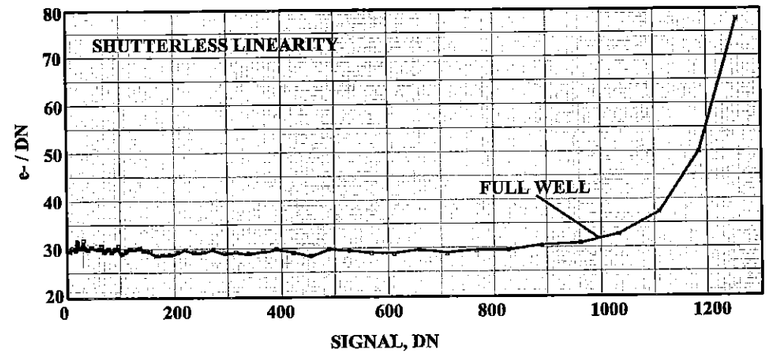

Figure 2.11(c) Linearity transfer curve based on the shutterless photon transfer method.

Solution:
From Eq. (2.22),

$$LR = 100 \times \{1 - 10^4/[(4.9 \times 10^3)/0.5]\},$$

$$LR = -2.04\%.$$

It should be mentioned that good linearity performance may still be seen beyond full well conditions. For example, linearity is well behaved when the average signal is measured about a small overexposed point source that has bloomed. Only when bloomed charge escapes the region being averaged will linearity suffer, because charge is conserved. This situation is different compared to a flat-field exposure where blooming takes place over the entire array. Here, the onset of nonlinearity and full well will occur at the same signal level. The camera gain constant (e^-/DN) can be plotted against signal to circumvent setup problems like this. This is because gain (e^-/DN) is dependent on both signal and noise [i.e., Eq. (2.8)]. Linearity measured in this manner is very sensitive to charge sharing between pixels. This measurement technique, combined with the shutterless photon transfer method described below, represents a powerful calibration tool in characterizing gain and linearity simultaneously without exposure time information. Figure 2.11(c) shows a linearity transfer curve based on this method.